Polymer 50 (2009) 5828–5836

Contents lists available at ScienceDirect

Polymer

journal homepage: www.elsevier.com/locate/polymer

Electrospinning nanoribbons of a bioengineered silk-elastin-like protein (SELP) from water

Yogesh Ner [a], Jeffrey A. Stuart [a,b], Gregg Whited [c], Gregory A. Sotzing [a,b,*]

[a] The Polymer Program, Institute of Materials Science, University of Connecticut, 97 N. Eagleville Rd., Storrs, CT 06269, USA
[b] Department of Chemistry, University of Connecticut, 97 N. Eagleville Rd., Storrs, CT Q1 06269, USA
[c] Genencor International, Inc., Palo Alto, CA 94304, USA

ARTICLE INFO

Article history:
Received 27 May 2009
Received in revised form
2 September 2009
Accepted 6 September 2009
Available online 12 September 2009

Keywords:
Silk-elastin-like protein
Electrospinning
Nanoribbons

ABSTRACT

Electrospinning of a silk-elastin-like protein (SELP), a repeat sequence protein polymer (RSPP) from aqueous solution, is reported here. The electrospinning of SELP47K resulted in fibers with a uniform, ribbon-like morphology. The solution properties of SELP47K provide ideal conditions for electrospinning and resultant nanoribbons are demonstrated to form self-standing, non-woven fiber meshes. The mechanical properties of these meshes have also been evaluated, and the ultimate tensile strength was found to be 30.8 MPa with an average initial modulus of 0.88 GPa. Furthermore, the effect of electrospinning parameters, such as solution concentration, applied voltage, collecting distance, and rate of spinning, on the fiber dimensions and morphology are studied. Within the experimental matrix, the width of these nanoribbons is found to be between 25 nm and 1800 nm. The secondary structure of SELP47K nanoribbons is analyzed by FTIR and WAXD and the methanol treatment resulted in improvements in the crystalline β-sheet structure when compared to as spun electrospun nanoribbons.

1. Introduction

The field of advanced functional biomaterials constitutes a relatively new discipline that blends traditional materials research with the unique properties inherent to biological molecules. Natural selection and evolution have endowed biological molecules with an almost unprecedented integration of structure and function, far beyond what is currently possible through *de novo* synthetic techniques. As such, biomolecules represent a novel toolkit for the fabrication of hybrid materials, with functions which are not possible to achieve through conventional means. The continuous efforts from biologists and material scientists are being made to design biomaterials that can offer self assembly, higher structural regularities, biocompatibility and catalytic and binding properties. Synthesizing repeat sequence protein polymers (RSPPs) of natural protein motifs offers a promising route to develop high performance polymers from the library of monomers e.g. small peptide-based RSPPs. Using a bottom up approach, various RSPPs of natural protein motifs such as elastin (GVGVP, VPGG, APGVGV), silk fibroin (GAGAGS), flagelliform silk (GPGGx), dragline silk (GPGQQ, GPGGY, GGYGPGS), collagen (GAPGAPGSQGAPGLQ, GAPGTPGPQGLPGSP), and keratin (AKLKLAEAKLELA) are possible. It is also possible to synthesize their block copolymers to combine material properties of two or more natural motifs, which can possess properties not found in either synthetic homoblock RSPPs. RSPPs have been studied as an alternative material to the natural analogues for the applications such as controlled drug delivery systems, tissue replacement and tissue engineering [1–3].

SELP, or silk-elastin-like Protein, is one of the successful series of genetically-engineered RSPP block copolymers consisting of silk and elastin protein subunits in defined ratios [4]. The biosynthesized block copolymers consist of silk-like (GAGAGS) and elastin-like (GVGVP) repeating units. The silk-like block mimics its natural analogue to assemble into tightly packed secondary structures, β-sheets, imparting strength to the protein polymer. Along with its inherited rubber like behavior, introduction of periodic elastin-like blocks reduces overall crystallinity of the system and increases water solubility. Genetically engineered SELP polymers are synthesized using recombinant techniques which enable precise control over molecular weight, sequence and composition and hence monodispersed polymer architecture with tailored biological, physicochemical, and material properties are possible. Several combinations of genetically engineered SELP block polymers which are important for biomedical applications have been

* Corresponding author. The Polymer Program, Institute of Materials Science, University of Connecticut, 97 N. Eagleville Rd., Storrs, CT Q1 06269, USA. Tel.: +1 860 486 4619; fax: +1 860 486 4745.
E-mail address: sotzing@mail.ims.uconn.edu (G.A. Sotzing).

0032-3861/$ – see front matter © 2009 Elsevier Ltd. All rights reserved.
doi:10.1016/j.polymer.2009.09.017

reported in literature [2,4–6]. These block copolymers have been reported to have molecular weights between 30 kDa and 250 kDa and have the ability to self assemble to form films, fibers and hydrogels. SELP also exhibits irreversible sol-to-gel transitions induced by heating or by long-term storage at room temperature. This phase transition can be tuned by temperature, pH, ionic strength and polymer concentration [7,8] or by varying the block ratio of silk to elastin [9] e.g SELP block copolymer having four silk-like (GAGAGS), seven elastin-like (GVGVP) repeating units with one of the elastin unit is modified with lysine, a.k.a. SELP47K, undergoes an irreversible sol-to-gel transition when transferred from room temperature to body temperature. In this composition, the lysine provides a convenient reactive site for modifications such as cross-linking. SELPs are biocompatible and have been extensively studied for encapsulation and controlled release of bioactive agents such as drugs, proteins, DNA, and adenoviral particles [2,4–6]. The various SELPs also have the ability to form self-standing films by solvent evaporation at room temperature, which exhibits high modulus and strength due to the presence of ordered β-sheets. Mechanical properties have been reported for films of SELP47K: 1.7 GPa modulus, 69.9 MPa tensile strength, and 8.4% elongation at break [10]. These values are similar to those of several high strength synthetic polymers, including high-density polyethylene and Nylon-6. The glass transition and decomposition temperatures of SELP47K are 189 °C and 332 °C respectively. High mechanical properties, water solubility, and biocompatibility make SELPs unique materials for bioencapsulation. SELP has also been shown to form strong interactions with embedded enzymes: glucose oxidase (GOx) suspended in dried SELP thin films did not leach after 28 h in a pH 6.5 buffer. At pH 7.6, GOx was released in a controlled manner. In both cases, no enzyme degradation was observed, and GOx activity was maintained at initial levels throughout the study [10]. Apart from encapsulation of bioactive/therapeutic agents, it is also possible to introduce functional peptides in the polymer sequence for various non-conventional applications of RSPPs [11].

Fibers of SELP polymers can be interesting candidates for applications in artificial muscles and scaffolds, artificial enzyme fibers, biosensors, environmental cleanup, wound dressing, drug delivery and protection materials. In the past, SELP block copolymers have been drawn into fiber using a solution extrusion technique utilizing high chaotropic solvents such as hexaflouro-2-propanol (HFIP) or formic acid as a solvent and various coagulant systems [12]. However, this results in restrictions for incorporation of a vast variety of functional water stable and soluble biomaterials. Recently, electrospinning has been extensively explored to produces fibers from protein polymers mainly due to its ability to form nanofibers with very high surface area [13,14]. It also offers control over fiber morphology, fiber alignment and the incorporation of functional materials. All these, combined with the simplicity and scalability of the process makes it ideal for many applications [15–22]. The process of electrospinning involves charging the polymer solution in a suitable solvent to a very high potential. At the threshold potential, a charged jet forms between the electrodes. Polymer solution travels along the path of jet, evaporating the solvent, leaving behind polymeric nanofibers on one of the electrodes (the collector). Electrospinning of several commodity and high performance polymers, including protein fibers, for a wide range of applications has been reported in literature [16,23–26]. Silk based electrospun nanofibers remain as an interest of many scientific studies because of their potential applications, taking advantage of both unique properties of silk and high surface area of nanofibers. The nanofibers are successfully made from regenerated natural silk [27–30]. However, often, the use of strong solvents such as hexaflouro-2-propanol (HFIP) or formic acid is necessary to make the spinning dope used for electrospinning. This restricts the incorporation of a vast variety of functional, water stable, and soluble biomaterials. Various other strategies have been applied to electrospin silk protein from non-malignant solvents. Most significant among them are dual spinnerets electrospinning [31,32] and blending another water soluble polymer in the spinning dope to facilitate spinning procedure, subsequently removing the carrier polymer by water treatment [33,34]. Using a similar strategy, blends of natural polymers, keratin, with regenerated silk have also been used for electrospinning [35]. Regenerated silk fibroins have also been reported to spin directly from aqueous solutions. However, reported mechanical properties are not adequate for many potential applications [35,36]. Another route to obtain high quality protein fiber utilizes RSPPs such as SELP47K. Genetically-engineered protein polymers containing silk or elastin-like sequences have been electrospun previously. Stephens et al. electrospun dragline spider silk analogues using HFIP as a solvent and observed changes in secondary structure in the electrospun fibers [37]. A (nano-) ribbon-like morphology was observed upon electrospinning a genetically-engineered elastin-like protein (ELP) polymer at a concentration of 15% (w/w) in water [38,39]. Recently, Nagarajan et al. reported electrospinning of SELP67K using HFIP as a solvent, or at aqueous concentrations higher than 7% with addition of surfactants and PEO [40]. Addition of PEO and surfactant leads to polymer micelle formation and thereby facilitates the process of fiber formation from aqueous solution. However, to the date no study indicating formation nanofibers from aqueous silk based RSPPs is reported.

With the aim of developing precursors for scaffold and drug delivery systems from high performance protein polymers, the present study reports electrospinning of SELP47K directly from aqueous solution without the addition of any external surface modifying agent. The electrospinning of SELP47K resulted in quasi-one dimensional nanoribbons. Electrospinning parameters have been studied to control the width of the nanoribbons and it has been demonstrated that protein ribbons with varying width from 20 nm to 1.8 μm can easily be achieved. The mechanical properties of the resultant ribbons are also evaluated and a breaking strength of 30.8 MPa and a modulus of 0.88 GPa were obtained. The secondary structure of the electrospun fibers are also evaluated using FTIR and WAXD.

2. Experimental

2.1. Materials

Silk-elastin-like protein used in the present study, termed as SELP47K, is a block copolymer having four silk-like (GAGAGS), seven elastin-like (GVGVP) repeating units with one of the elastin units modified with lysine. The letter indicates sequence of amino acid, G-glycine, A-alanine, S-serine, V-valine, P-proline, K-lysine. Fig. 1 shows the repeating block structure of SELP47K. The polymer was obtained from Genencor International and used as received. The detailed synthetic procedure is described elsewhere [4,11]. The molecular weight of the polymer is 84,000 Da.

2.2. Electrospinning

For the present study, the experimental set-up similar to our previous studies was used [41–43]. It consists of 3 mL syringe with 24 gauge blunt tip needle containing SELP47K solution positioned

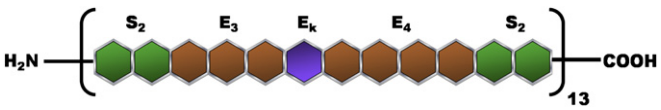

Fig. 1. Unit blocks of SELP47K, S = silk protein sequence, E = elastin protein sequence, K = lysine modified elastin protein sequence.

above a copper plate collector. Polymer solution was obtained by mixing appropriate amounts of SELP47K in deionized water (Millipore 18 MΩ). After complete dissolution of polymer, the solutions were stored at 4 °C and allowed to come to room temperature for 30 min before electrospinning. Nanofibers are collected either on aluminum glass mirrors or aluminum foil by placing these secondary collectors on the copper plate collector. The temperature and humidity of the electrospinning chamber was at 23 ± 2 °C and 55 ± 5% respectively.

2.3. Design of experiment

"One Factor at a Time" approach is followed to determine effect of electrospinning process variables on fiber morphology and fiber diameter. Four major factors which determine fiber diameter and fiber morphology, solution concentration, applied voltage, collecting distance and rate of spinning are considered during the study. Solution concentrations are varied from 6% to 18% (w/w). The rate of spinning is controlled by adjusting the flow of the SELP47K solution using motorized syringe pump between 0.1 mL/h and 1.6 mL/h. Distance between collector and syringe needle assembly is varied between 10 cm and 20 cm. Finally, the applied voltage was varied from 10 kV to 20 kV.

2.4. Methanol treatment of electrospun mats

As-spun SELP47K non-woven fiber meshes were immersed in a methanol solution for 10 min. After treatment the fiber mesh was dried at room temperature for 24 h, before any characterization.

2.5. Polarized Light Microscopy (PLM)

The PLM experiments were performed on the fibers deposited on the plain glass slide using an Olympus BX51P microscope.

2.6. Mechanical properties of nanofiber meshes

Stress–strain properties of SELP47K nanofiber meshes were measured with a TA Instruments Dynamic Mechanical Analyzer (DMA2980) in the tensile (film) mode at 23 °C. As-spun self-

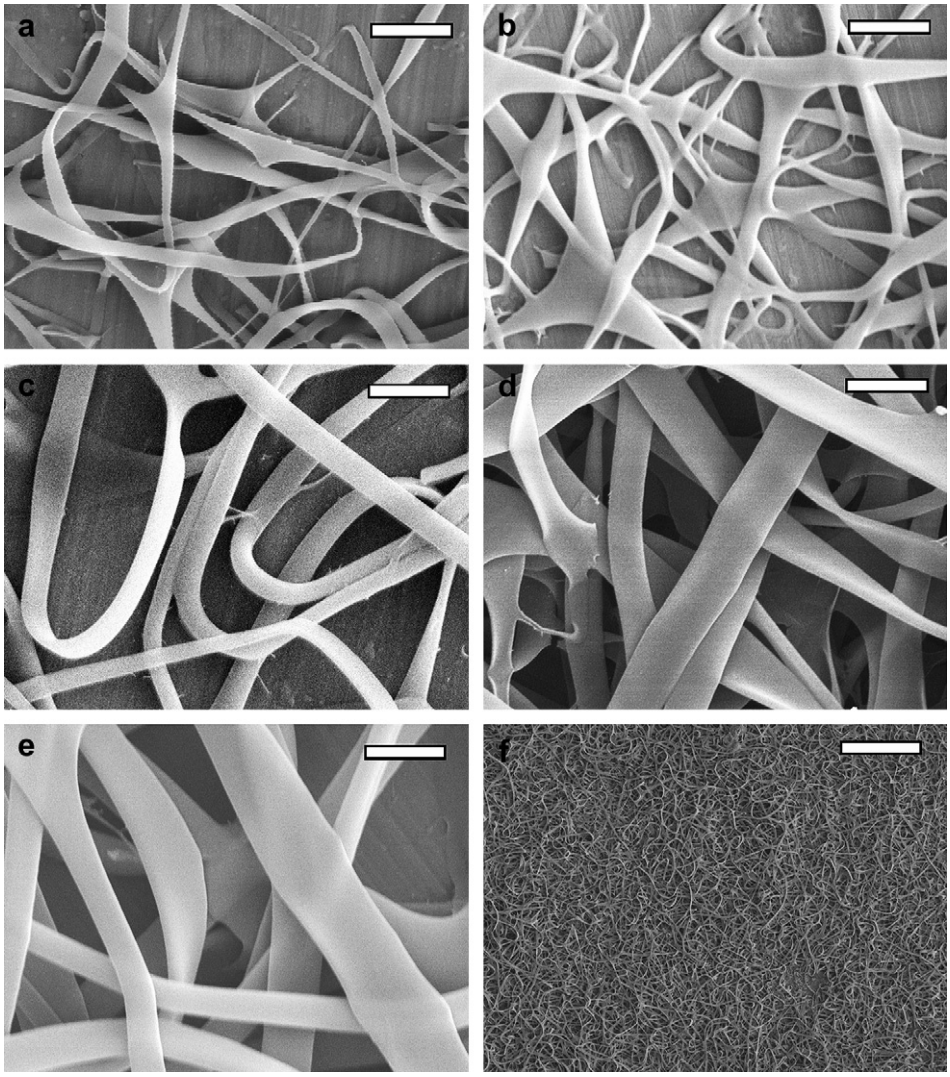

Fig. 2. FESEM images of nanoribbons obtained by electrospinning from aqueous solution at various concentrations of SELP47K 6% (a), 9% (b), 12% (c), 15% (d), 18% (e) (w/w) and low magnification image at 15% (f), other electrospinning conditions were kept at a constant applied voltage (20 KV), collecting distance (15 cm) and flow rate (0.1 mL/h). (Scale bar – a–e: 1 μm, f: 25 μm).

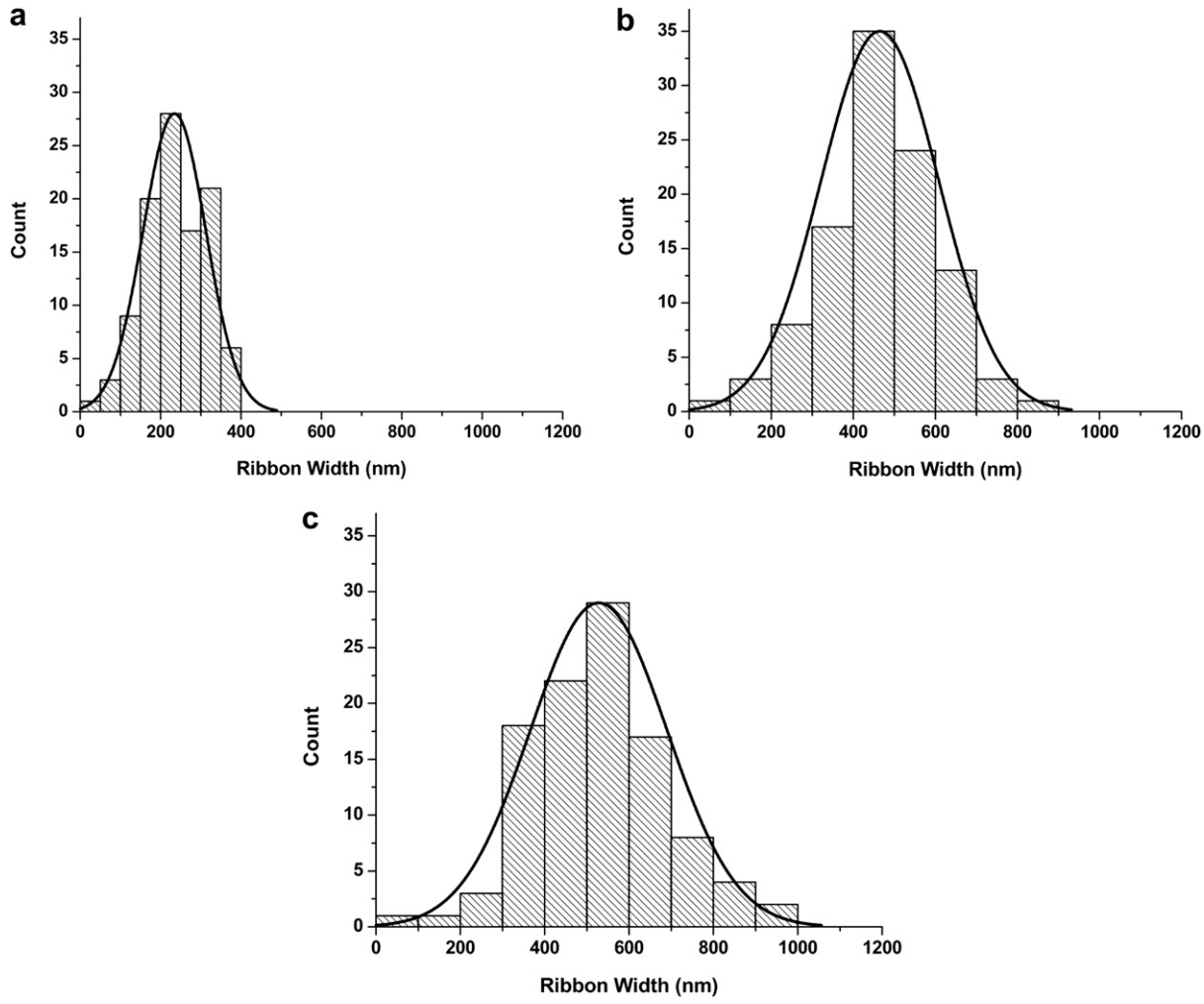

Fig. 3. Flat ribbon width distribution at various concentrations (w/w) 12% (a), 15% (b) and 18% (c).

standing non-woven meshes were cut into rectangular strips (10×30 mm) and mounted on a paper template which is used to provide a stronger gripping surface during the test. The tests were carried out at test speed of 1 mN/min. Sample thicknesses were measured using a Zygo 3-D Optical Scanning Interferometer. The reported results are average values from 3 test samples.

2.7. Field Emission Scanning Electron Microscope (FESEM)

The electrospun fibers were collected on aluminum foil and sputtered coated for 2 min prior to imaging using the JEOL 6335F FESEM. The average fiber diameter and its distribution were determined based on analysis of 100 randomly selected fibers from

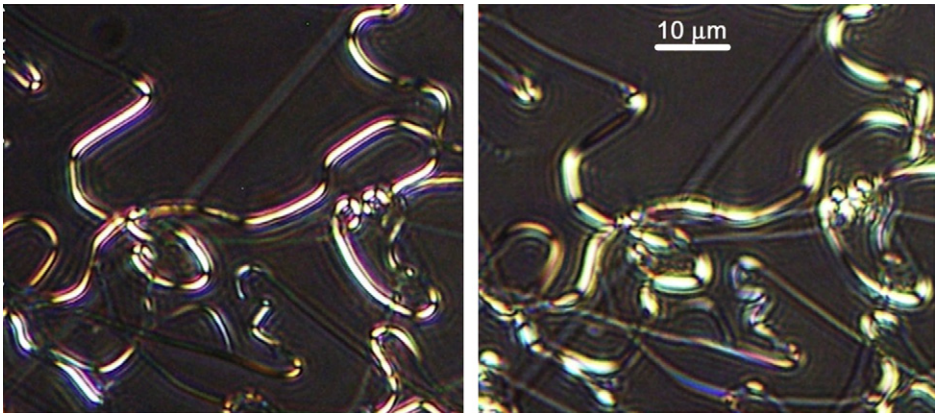

Fig. 4. Birefringence of SELP47K nanoribbons observed under cross polarized light by rotating the sample by 45°.

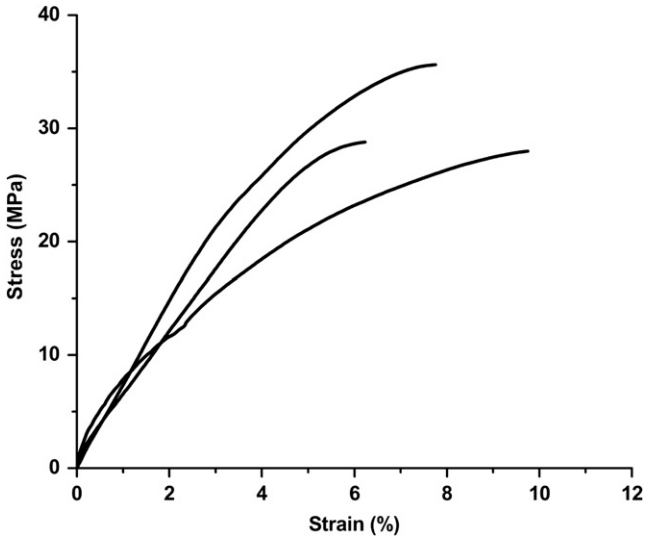

Fig. 5. Stress–strain behavior of electrospun SELP47K self standing nanoribbons meshes prepared from 15% (w/w) aqueous solution.

at least 10 images obtained from each spinning condition using *ImageJ* image processing program. For all samples, time of spinning was kept constant at 2 min and for imaging 5 × 5 mm pieces from the center of the aluminum foil collector were used.

2.8. FTIR

IR characterization was carried out using Nicolet Magna 560 FTIR spectrometers with microscope attachment. Fibers were collected on the aluminum mirror surface and were analyzed in reflectance mode. Using FTIR-microscopy, The IR beam was positioned at a known position in the fiber samples. All spectra were acquired by adding 64 scans with a resolution of 4 cm^{-1} between the spectral range of 4000–650 cm^{-1}.

2.9. X-ray diffraction

WAXD experiments were performed on Xcalibur PX Ultra diffractometer (Oxford Diffraction) with sample to Onyx CCD detector distance of 65 mm using the CuKα radiation (wavelength $\lambda = 0.154$ nm).

3. Results and discussion

3.1. Electrospinning and fiber morphology

Initial experiments of the electrospinning of SELP47K aqueous solution is carried out by varying solution concentration of the spinning dope. Although the protein polymer is highly water soluble, it has a tendency to form a gel irreversibly. Gelation of the protein polymer solution may cause problems in the electrospinning process. The rate of gelation of the SELP polymers can be

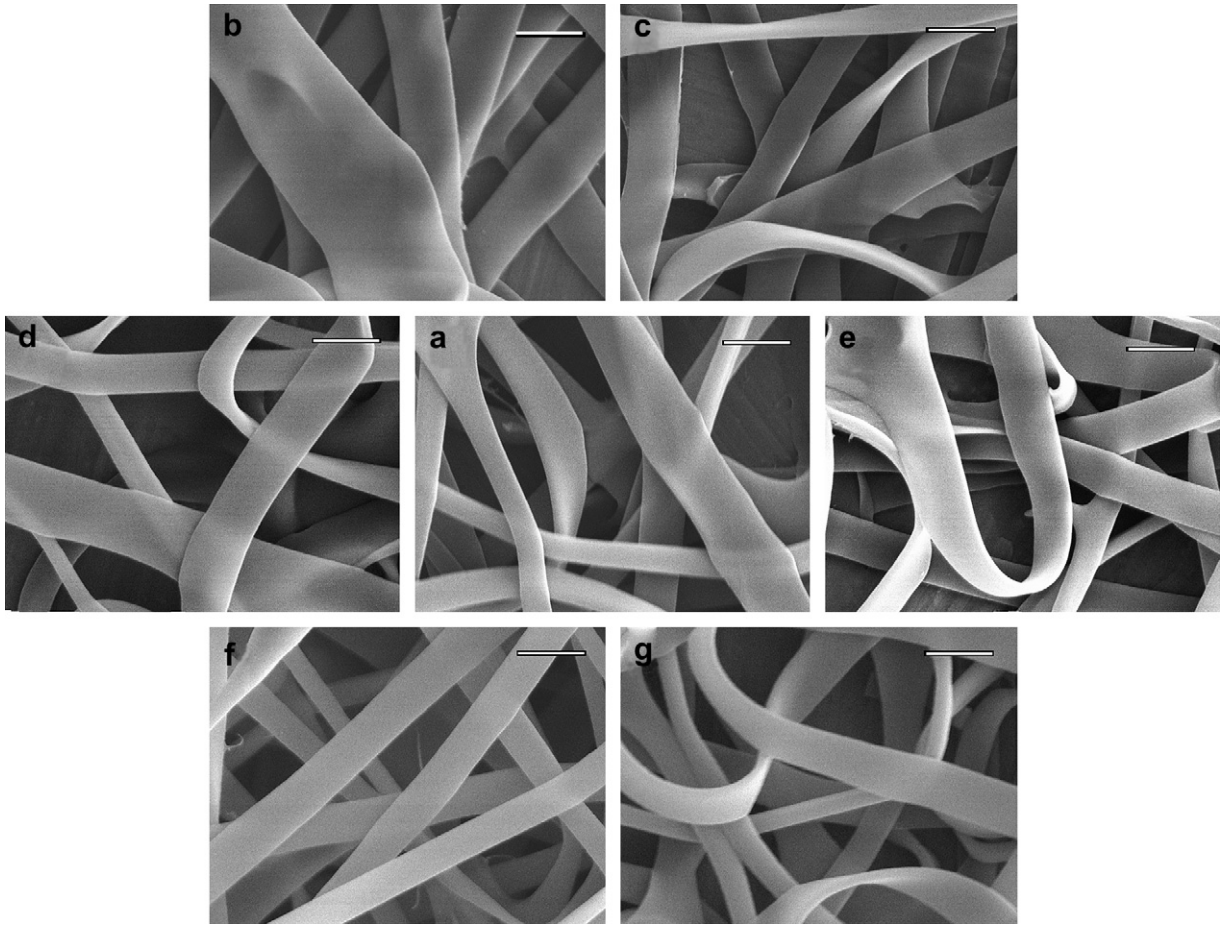

Fig. 6. Effect of electrospinning parameters on the nanoribbons morphology from 18% aqueous solution, Control applied voltage (20 kV), collecting distance (15 cm) and flow rate (0.1 mL/h) (a), Effect of applied voltage 10 kV (b), 15 kV (c), Effect of collecting distance 10 cm (d), 20 cm (e), Effect of flow rate 0.8 mL/h (f) and 1.6 mL/h (g) (Scale bar −1 μm).

Table 1
Statistical analysis of the nanofiber ribbons obtained from the FESEM images (sample size = 100 fibers for each condition).

Concentration	Applied voltage (kV)	Flow rate (mL/h)	Collecting distance (cm)	Average fiber width (nm)	Standard deviation	Maximum fiber width (nm)	Minimum fiber width (nm)
12%	20	0.1	15	238	72	391	92
	10	0.1	15	No fiber obtained			
	15	0.1	15	255	103	629	56
	20	0.1	10	No data collected			
	20	0.1	20	221	87	473	25
	20	0.8	15	No data collected			
	20	1.6	15	216	78	399	68
15%	20	0.1	15	472	129	800	197
	10	0.1	15	No fiber obtained			
	15	0.1	15	557	155	882	177
	20	0.1	10	473	140	967	60
	20	0.1	20	432	162	774	75
	20	0.8	15	490	150	735	79
	20	1.6	15	530	159	1383	220
18%	20	0.1	15	535	144	963	247
	10	0.1	15	833	243	1805	383
	15	0.1	15	675	175	1099	265
	20	0.1	10	574	154	976	80
	20	0.1	20	503	186	977	162
	20	0.8	15	533	189	1092	184
	20	1.6	15	584	216	1593	271

decreased either by decreasing the solution concentration or by lowering the storage temperature. However, lowering polymer concentration can hamper formation of a stable Taylor cone, which is required for the formation of uniform fibers. At higher concentrations, the rate of gelation is faster and may lead to solutions that cannot be electrospun. Considering these aspects, the experiments are carried out with the solution concentrations varied between 6 and 18% (w/w). In this concentration range, SELP47K solution can be stored at room temperature for at least 3 h without any observable gelation.

Fig. 2 shows representative FESEM images of the fiber morphology of SELP47K fibers at various concentrations from 6% (w/w) to 18% (w/w). In all cases, other electrospinning parameters *i.e.* applied voltage (20 kV), collecting distance (15 cm) and flow rate (0.1 mL/h) are kept constant. Irrespective of the solution concentration, electrospinning of SELP47K resulted in flat, ribbon-like morphology. The flat ribbon formation can be described by the formation of thin skin around the electrospinning liquid jet due to rapid evaporation of the solvent from the surface as compared to the fiber core. This results in polymeric tubes carrying solution which collapse at the collector to form a flat, ribbon-like morphology [44,45]. It has been observed previously that polymers having tendency to form strong intra- and inter-chain interactions can form semi-crystalline microgel particles in their solutions and electrospinning of these solutions can result in flat fibers. The formation of gel domains may be accelerated during solvent evaporation [46]. In the case of SELP47K aqueous solutions, silk-like blocks can crystallize to form β-sheets, surrounded by solvated elastin blocks. This may explain the formation of nanoribbons even at low solution concentrations.

At low concentrations, 6% and 9%, very often fiber splitting is also observed, which results in triangle-shaped bifurcated fibers. The fiber splitting is a result of ejection of smaller jets from the primary jet comparable to the ejection of a primary jet from the charged droplet. During the travel of the primary jet towards the collector, both the charge density and local polymer concentration changes resulting in local instabilities. These instabilities can be minimized by ejecting smaller jets resulting in branched fibers. The tendency to form branched fibers has been observed to decrease with increasing concentration. At higher concentration, the secondary jet ejection can be prevented by higher local concentration of polymer chains in the primary jet minimizing local instability by avoiding solvent congregation [44,45,47,48]. Upon increasing the concentration, above 12%, uniform morphology and continuous flat ribbons are formed. Thus, the viscosity and surface tension of SELP47K aqueous solution are suitable to generate the uniform Taylor cone that is required for continuous spinning.

Fig. 2F shows a low magnification image of the electrospun SELP47K mat; the ribbons are distributed uniformly across the surface. Fig. 3 depicts the fiber size distribution, resulting from image analysis of 100 random nanoribbons from the non-woven mesh of SELP47K spun at concentration of 12%, 15% and 18% (w/w). Under the experimental conditions, the average fiber diameter was found to be 238 nm, 472 nm and 535 nm respectively. With increasing solution concentration, broader fiber size distributions are observed.

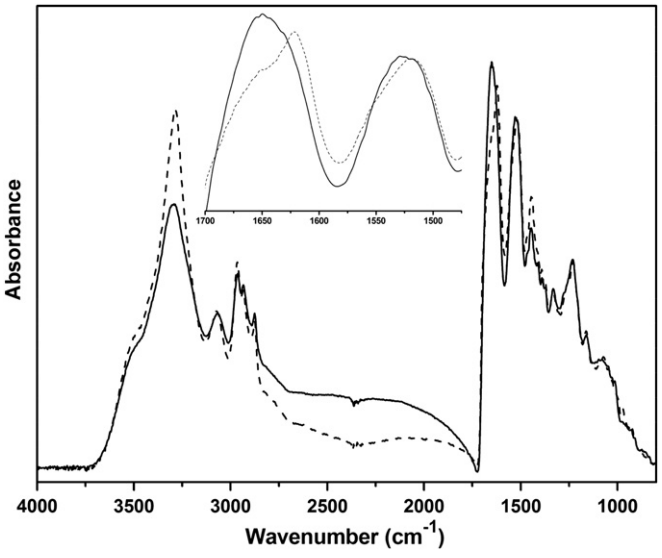

Fig. 7. FTIR spectra of SELP47K nanoribbons as spun fibers (dashed line) and after methanol treatment (dotted line).

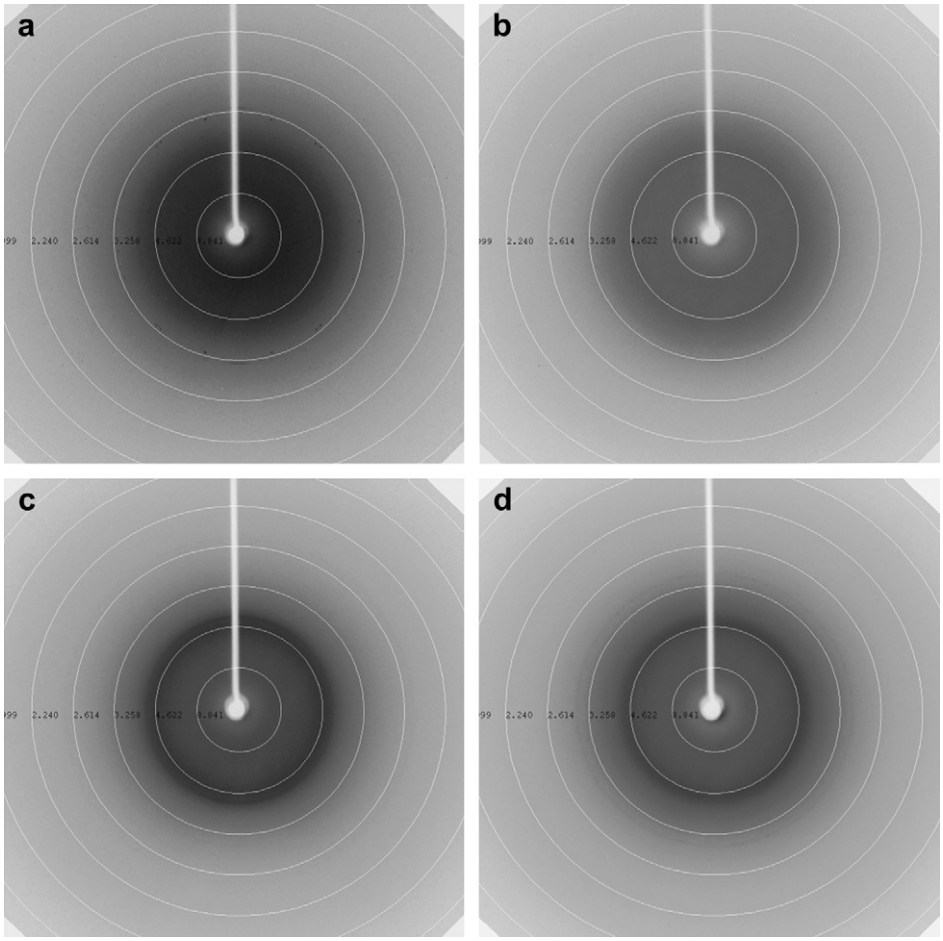

Fig. 8. WAXD pattern of SELP47K, as spun electrospun mat (a), film (b), methanol treated electrospun mat (c) and methanol treated film (d).

The RSPP SELP47K has been designed to carry functions from both constituting blocks of the native protein into the recombinant derivative. Silk blocks and elastin blocks are expected to assemble into regular secondary structures in the fibers. Fig. 4 shows optical micrographs of SELP47K nanofibers under cross polarizer observed by clockwise rotating sample by 45°. The fibers demonstrate birefringence, indicating the presence of regularity owing to chain orientation. The change in dark and bright segment was also observed by clockwise rotating the sample by 45°. In previous studies, the triblock copolymer styrene-butadiene-styrene showed similar behavior [49]. Fig. 4 also shows a view of several bent nanoribbons resulting from an electrically driven bending instability.

3.2. Mechanical properties of nanoribbons

A characteristic uniaxial stress–strain curves of dried SELP47K nanoribbons with average sample thickness of 20 μm are shown in Fig. 5. The average ultimate tensile strength of samples is found to be 30.8 MPa, with an average initial modulus of 0.88 GPa; strain values are 7.9%. The values reported here are for dried samples and can be significantly improved by methanol treatment or by cross-linking [34,36].

3.3. Controlling fiber dimensions

Several factors such as solution properties, environmental factors, and electrospinning process parameters can play a major role in determining fiber morphology, size and distribution. Within the experimental matrix of the present study, electrospinning process parameters such as flow rate, collecting distance and spinning voltage are considered as the major determinants of the ribbon size and distribution. This experimental matrix is expected to provide information for achieving controlled fiber diameter which can be crucial for designing fibers for specific target applications, e.g. encapsulation of proteins with varied sizes. Fig. 6 shows SELP47K nanofiber ribbons spun from 18% aqueous solution under various electrospinning conditions. Table 1 represents the experimental matrix and the statistical analysis of the nanofiber ribbons obtained from the FESEM images. Within the set of experiments, nanoribbons with diameters ranging from 25 nm to 1805 nm were obtained. As explained earlier, increasing solution concentration resulted in an increase in fiber width. Increasing solution feed rate also resulted in an increase in the fiber width. This can be explained on the basis of increases in the spinnable protein solution volume at the needle tip [50,51]. Increasing collecting distance has two simultaneous effects which can play role in determining fiber dimensions: decreasing field strength and increasing time of flight of the fiber. In our case, the ribbon width is found to decrease with increasing collecting distance. At lower concentrations, 12% and 15%, no significant fiber formation is observed at low voltage (10 kV). Increasing the voltage from 10 kV to 15 kV, holding all other parameters constant at 12% and 15% concentration, resulted in a stable Taylor cone and thereby formation of uniform nanoribbons on the collector. At 18% concentration, formation of a uniform Taylor cone even at a lower

voltage, 10 kV, was observed. Within all experimental conditions, flat nanoribbons are formed and, in general, increasing voltage decreased the nanoribbons width. Both solution concentration and applied voltage have a dominant role in controlling nanoribbon width. The effect of gelation and solvent might be crucial in terms of deciding both fiber morphology and dimension; no attempts have been made to study these effects. However, compared to previous approaches for spinning SELP family proteins from water by adding surface modifying agents such as PEO and surfactants [40], our study indicates that with proper selection of the protein polymer and electrospinning parameters, high quality protein fibers can be obtained without the addition of any external agents. Furthermore, efforts are also being made to understand the role taken by solution properties and by the protein polymer on ribbon formation.

3.4. Secondary structure of electrospun SELP47K ribbons

Previous studies have shown that electrospun silk based fibers prepared both from aqueous [34,36] or organic solvents [27] resulted in amorphous structure with predominantly a random coil conformation. This was attributed to the slower crystallization rate of the silk β-sheet compared to the rapid evaporation of the solvent during electrospinning limiting the molecular rearrangement required for crystallization. Subsequent methanol treatment of electrospun nanofiber mats resulted in improved β-sheet structure. FTIR is often utilized to characterize the major conformations of silk, including- random coils (silk I) and β-sheets (silk II). The characteristic FTIR absorption bands for amorphous random coils are at 1655 (amide I), 1540 (amide II), and 1235 cm^{-1} (amide III), and β-sheet conformation is characterized by absorption bands at 1628 (amide I), 1533 (amide II), and 1265 cm^{-1} (amide III) [52]. Fig. 7 shows FTIR spectra of the as-spun SELP47K fibers compared to methanol treated fibers. In the case of SELP47K, as spun fibers show adsorption bands at 1651, 1528 and 1230 cm^{-1}, attributed to the presence of random coil conformations. Upon methanol treatment, the fiber mats show strong absorption bands at 1622, 1520 and 1261 cm^{-1}, indicating improvement in the β-sheet content.

These results were confirmed by wide-angle X-ray diffraction (WAXD), Fig. 8, where as-spun nanoribbons, and methanol treated nanoribbons are compared to thin films of same composition and treatment. In the case of as-spun ribbons and thin films, a broad distributed pattern with a peak at $2\theta = 16.1^\circ$ was observed. This might be due to the predominant presence of random coil conformation. However, this cannot be attributed to the rapid evaporation of the solvent during electrospinning as films which are prepared at slower rates of evaporation also showed similar behavior. Upon methanol treatment for 10 min, both films and fibers showed sharp Bragg reflection peaks at $2\theta = 20.1^\circ$, clearly indicating formation of the β-sheet structure. Thus, the native structure of the SELP47K in aqueous solution is preserved during electrospinning. It might be interesting to investigate effects of solvent on the secondary structure, as SELP47K can be spun either from aqueous solution or from organic solvents. However, this is beyond the scope of our interest, which is directed towards utilizing SELP47K for encapsulating biological agents or using these nanofibers for scaffold applications.

4. Conclusions

In conclusion, we have shown that SELP47K can be electrospun from aqueous solutions without the addition of any external agent. This is a significant advance, in that it enables the incorporation of water-soluble or dispersible compounds that are otherwise unstable in organic solvents into protein nanofibers. The electrospinning of aqueous SELP47K solution shows typical electrospinning behavior of nanoribbon forming polymers wherein at lower spin dope concentrations the formation of triangle-shaped bifurcated fibers is observed. The formation of nanoribbons could result in a significant strategic advantage for encapsulation of enzymes and other quasi-one dimensional flat structures, where their activity is detected by maximum surface contact with the analytes. Interestingly, Hou et al. reported improved optical properties of microbelts over nanofibers and attributed to increase in surface area along with nearly defect free structure of one dimensional ribbons [53].

Within the experimental matrix of the present study, the width dimension of SELP47K nanoribbons can be controlled from a few nanometers to a few microns. This enables us to choose spinning parameters to produce nanostructures with the desired dimensions, and it is also possible to produce fibers that are orders of magnitude smaller than most natural fibers (~2–5 μm). The mechanical properties, along with the biocompatibility and self standing nature of the SELP47K nanoribbons are sufficient enough to use for tissue engineering applications [25]. The post treatment, such as cross-linking of pendant lysine group, alcohol treatment for enhancing β-sheet content could impart water insolubility as well as enhanced mechanical properties to these ribbons. In all, this study strengthens our efforts for constructing and utilizing biologically based nanofibers for encapsulating enzymes, proteins and therapeutic agents.

Acknowledgment

The authors are thankful to Genencor Int. for their technical support and their supply of SELP used for this work. GAS acknowledges the National Science Foundation (DMR 0502928) for financial support of this project. We would also like to acknowledge help from Gary Lavigne, Jack Gromek and Shih-po Sun for FTIR, XRD and mechanical characterization, respectively.

References

[1] Chow D, Nunalee ML, Lim DW, Simnick AJ, Chilkoti A. Materials Science and Engineering R, Reports 2008;62(4):125–55.
[2] Megeed Z, Haider M, Li D, O'Malley Jr BW, Cappello J, Ghandehari H. Journal of Controlled Release 2004;94(2–3):433–45.
[3] Huang J, Wong Po Foo C, Kaplan DL. Polymer Reviews 2007;47(1):29–62.
[4] Megeed Z, Cappello J, Ghandehari H. Advanced Drug Delivery Reviews 2002;54(8):1075–91.
[5] Haider M, Leung V, Ferrari F, Crissman J, Powell J, Cappello J, et al. Molecular Pharmaceutics 2005;2(2):139–50.
[6] Megeed Z, Cappello J, Ghandehari H. Pharmaceutical Research 2002;19(7):954–9.
[7] Nagarsekar A, Crissman J, Crissman M, Ferrari F, Cappello J, Ghandehari H. Biomacromolecules 2003;4(3):602–7.
[8] Nagarsekar A, Crissman J, Crissman M, Ferrari F, Cappello J, Ghandehari H. Journal of Biomedical Materials Research 2002;62(2):195–203.
[9] Dinerman AA, Cappello J, Ghandehari H, Hoag SW. Biomaterials 2002;23(21):4203–10.
[10] Kumar M. Use of repeat sequence protein polymers in personal care compositions. US Patent, US 20050142094 A1, 2005.
[11] Kumar M, Sanford KJ, Cuevas WA, Du M, Collier KD, Chow N. Biomacromolecules 2006;7(9):2543–51.
[12] Cappello J, McGrath KP. Spinning of protein polymer fibers. In: Kaplan D, Adams WW, Farmer B, Viney C, editors. American Chemical Society Symposium Series 544; 1993. p. 311–41.
[13] Schiffman JD, Schauer CL. Polymer Reviews 2008;48(2):317–52.
[14] Venugopal J, Ramakrishna S. Applied Biochemistry and Biotechnology: Part A Enzyme Engineering and Biotechnology 2005;125(3):147–57.
[15] Burger C, Hsiao BS, Chu B. Nanofibrous materials and their applications. Annual Review of Materials Research 2006;36:333–68.
[16] Huang ZM, Zhang YZ, Kotaki M, Ramakrishna S. Composites Science and Technology 2003;63(15):2223–53.
[17] Kumbar SG, Nair LS, Bhattacharyya S, Laurencin CT. Journal of Nanoscience and Nanotechnology 2006;6(9–10):2591–607.
[18] Liang D, Hsiao BS, Chu B. Advanced Drug Delivery Reviews 2007;59(14):1392–412.

[19] Rutledge GC, Fridrikh SV. Advanced Drug Delivery Reviews 2007;59(14): 1384–91.
[20] Schreuder-Gibson H, Gibson P, Senecal K, Sennett M, Walker J, Yeomans W, et al. Journal of Advanced Materials 2002;34(3):44–55.
[21] Sill TJ, von Recum HA. Biomaterials 2008;29(13):1989–2006.
[22] Teo WE, Ramakrishna S. Nanotechnology 2006;17(14).
[23] Bognitzki M, Czado W, Frese T, Schaper A, Hellwig M, Steinhart M, et al. Advanced Materials 2001;13(1):70–2.
[24] Li D, Xia Y. Advanced Materials 2004;16(14):1151–70.
[25] Li WJ, Laurencin CT, Caterson EJ, Tuan RS, Ko FK. Journal of Biomedical Materials Research 2002;60(4):613–21.
[26] Reneker DH, Yarin AL, Fong H, Koombhongse S. Journal of Applied Physics 2000;87(9 I):4531–47.
[27] Ayutsede J, Gandhi M, Sukigara S, Micklus M, Chen HE, Ko F. Polymer 2005;46(5):1625–34.
[28] Zarkoob S, Eby RK, Reneker DH, Hudson SD, Ertley D, Adams WW. Polymer 2004;45(11):3973–7.
[29] Jeong L, Lee KY, Park WH. Key Engineering Materials 2007;342–343:813–6.
[30] Alessandrino A, Marelli B, Arosio C, Fare S, Tanzi MC, Freddi G. Engineering in Life Sciences 2008;8(3):219–25.
[31] Yu HJ, Fridrikh SV, Rutledge GC. Advanced Materials 2004;16(17):1562–6.
[32] Wang M, Yu JH, Kaplan DL, Rutledge GC. Macromolecules 2006;39(3): 1102–7.
[33] Jin HJ, Fridrikh SV, Rutledge GC, Kaplan DL. Biomacromolecules 2002; 3(6):1233–9.
[34] Wang M, Jin HJ, Kaplan DL, Rutledge GC. Macromolecules 2004;37(18): 6856–64.
[35] Zoccola M, Aluigi A, Vineis C, Tonin C, Ferrero F, Piacentino MG. Biomacromolecules 2008;9(10):2819–25.
[36] Chen C, Chuanbao C, Xilan M, Yin T, Hesun Z. Polymer 2006;47(18):6322–7.
[37] Stephens JS, Fahnestock SR, Farmer RS, Kiick KL, Chase DB, Rabolt JF. Biomacromolecules 2005;6(3):1405–13.
[38] Huang L, McMillan RA, Apkarian RP, Pourdeyhimi B, Conticello VP, Chaikof EL. Macromolecules 2000;33(8):2989–97.
[39] Nagapudi K, Brinkman WT, Leisen JE, Huang L, McMillan RA, Apkarian RP, et al. Macromolecules 2002;35(5):1730–7.
[40] Nagarajan R, Drew C, Mello CM. Journal of Physical Chemistry C 2007;111(44):16105–8.
[41] Ner Y, Grote JG, Stuart JA, Sotzing GA. Soft Matter 2008;4(7):1448–53.
[42] Jang S-Y, Seshadri V, Khil MS, Kumar A, Marquez M, Mather PT, et al. Advanced Materials 2005;17(18):2177–80.
[43] Ner Y, Grote JG, Stuart JA, Sotzing GA. Angewandte Chemie International Edition 2009; 48(28):5134–38.
[44] Koombhongse S, Liu W, Reneker DH. Journal of Polymer Science, Part B: Polymer Physics 2001;39(21):2598–606.
[45] Reneker DH, Yarin AL. Polymer 2008;49(10):2387–425.
[46] Koski A, Yim K, Shivkumar S. Materials Letters 2004;58(3–4):493–7.
[47] Yarin AL, Kataphinan W, Reneker DH. Journal of Applied Physics 2005;98(6):064501.
[48] Holzmeister A, Greiner A, Wendorff JH. Polymer Engineering & Science 2008. ASAP article.
[49] Fong H, Reneker DH. Journal of Polymer Science, Part B: Polymer Physics 1999;37(24):3488–93.
[50] Zong X, Kim K, Fang D, Ran S, Hsiao BS, Chu B. Polymer 2002;43(16):4403–12.
[51] Zuo W, Zhu M, Yang W, Yu H, Chen Y, Zhang Y. Polymer Engineering & Science 2005;45(5):704–9.
[52] Um IC, Kweon HY, Lee KG, Park YH. International Journal of Biological Macromolecules 2003;33(4–5):203–13.
[53] Hou Z, Yang P, Li C, Wang L, Lian H, Quan Z, et al. Chemistry of Materials 2008;20(21):6686–96.